Dissecting the Catalytic Mechanism of Betaine−Homocysteine S -Methyltransferase by Use of Intrinsic Tryptophan Fluorescence and Site-Directed Mutagenesis †

ARTICLE *in* BIOCHEMISTRY · JUNE 2004

Impact Factor: 3.02 · DOI: 10.1021/bi049821x · Source: PubMed

7 AUTHORS, INCLUDING:

Carmen Castro
Universidad de Cádiz
31 PUBLICATIONS **874** CITATIONS
SEE PROFILE

Jirí Jirácek
Academy of Sciences of the Czech Republic
75 PUBLICATIONS **1,309** CITATIONS
SEE PROFILE

Michaela Collinsová
Academy of Sciences of the Czech Republic
16 PUBLICATIONS **331** CITATIONS
SEE PROFILE

Dissecting the Catalytic Mechanism of Betaine−Homocysteine *S*-Methyltransferase by Use of Intrinsic Tryptophan Fluorescence and Site-Directed Mutagenesis†

Carmen Castro,‡,§ Alejandra A. Gratson,‡ John C. Evans,|| Jiri Jiracek,⊥ Michaela Collinsová,⊥ Martha L. Ludwig,|| and Timothy A. Garrow*,‡

Department of Food Science and Human Nutrition, University of Illinois, Urbana, Illinois 61801, Biophysics Research Division and Department of Biological Chemistry, University of Michigan, Ann Arbor, Michigan 48109, and Department of Biological Chemistry, Academy of Sciences of the Czech Republic, 166 10 Prague 6, Czech Republic

Received January 23, 2004; Revised Manuscript Received March 9, 2004

ABSTRACT: Betaine−homocysteine *S*-methyltransferase (BHMT) is a zinc-dependent enzyme that catalyzes the transfer of a methyl group from glycine betaine (Bet) to homocysteine (Hcy) to form dimethylglycine (DMG) and methionine (Met). Previous studies in other laboratories have indicated that catalysis proceeds through the formation of a ternary complex, with a transition state mimicked by the inhibitor *S*-(δ-carboxybutyl)-l-homocysteine (CBHcy). Using changes in intrinsic tryptophan fluorescence to determine the affinity of human BHMT for substrates, products, or CBHcy, we now demonstrate that the enzyme−substrate complex reaches its transition state through an ordered bi-bi mechanism in which Hcy is the first substrate to bind and Met is the last product released. Hcy, Met, and CBHcy bind to the enzyme to form binary complexes with K_d values of 7.9, 6.9, and 0.28 μM, respectively. Binary complexes with Bet and DMG cannot be detected with fluorescence as a probe, but Bet and DMG bind tightly to BHMT−Hcy to form ternary complexes with K_d values of 1.1 and 0.73 μM, respectively. Mutation of each of the seven tryptophan residues in human BHMT provides evidence that the enzyme undergoes two distinct conformational changes that are reflected in the fluorescence of the enzyme. The first is induced when Hcy binds, and the second, when Bet binds. As predicted by the crystal structure of BHMT, the amino acids Trp44 and Tyr160 are involved in binding Bet, and Glu159 in binding Hcy. Replacing these residues by site-directed mutagenesis significantly reduces the catalytic efficiency (V_{max}/K_m) of the enzyme. Replacing Tyr77 with Phe abolishes enzyme activity.

There are two enzymes that have been characterized in mammals that methylate Hcy[1] to form Met; cobalamin-dependent methionine synthase (EC 2.1.1.13) and betaine−homocysteine *S*-methyltransferase (BHMT; EC 2.1.1.5). Both enzymes belong to a family of thiol/selenol methyltransferases (Pfam 02574) (*1*), and both require a zinc atom for the alkylation of the Hcy thiol (*2*, *3*). Sequence homologies predict that the rest of the family members also require zinc for catalysis since they share two small motifs that together contain the three Cys residues required for zinc binding in BHMT (*4*) and cobalamin-dependent methionine synthase (*5*). The crystal structures of human BHMT and of the N-terminal Hcy binding domain of cobalamin-dependent methionine synthase from *Thermotoga maritima* are very similar (*1*, *6*), which indicates that studies addressing the mechanism of these reactions may uncover catalytic features common to all Pfam 02574 members. The BHMT reaction and the structures of its substrates, products, and a bisubstrate analogue, *S*-(δ-carboxybutyl)-L-homocysteine (CBHcy), are shown in Figure 1.

Early studies of BHMT by Fromm and Nordlie (*7*) indicated that the steady-state kinetics were consistent with a reaction that proceeds through the formation of a ternary enzyme−substrate complex (*7*). These findings were supported later by the report (*8*) that CBHcy was able to inhibit BHMT at low micromolar concentrations. Product inhibition studies by Finkelstein et al. (*9*) suggested that the BHMT−Hcy−Bet ternary complex is formed by an ordered bi-bi mechanism in which Hcy is the first substrate bound and Met is the last substrate released.

It is generally recognized that enzymes cannot be regarded as rigid structures. If an enzyme reaction follows an ordered bi-bi mechanism, it is possible that the first substrate itself forms part of the binding site for the second substrate or drives conformational changes in the enzyme that create the second substrate binding site according to the "induced-fit" hypothesis of Koshland (*10*). In these cases, it would not be possible for the second substrate to bind in the absence of the first. However, an induced-fit mechanism has not been

† This research was supported by NIH Grants GM16429 (M.L.L.) and DK52501 (T.A.G.), by the Illinois Agricultural Experiment Station, Project ILLU-698-352 (T.A.G.), and by Grant A4055302 (J.J.) and Project Z4055905 (J.J.) from the Academy of Sciences of the Czech Republic.

* Corresponding author: 905 S. Goodwin Ave., Urbana, IL 61801. Phone (217) 333-8455; fax (217) 333-9368; e-mail tagarrow@uiuc.edu.

‡ University of Illinois.

§ Present address: Department of Biochemistry, University of Illinois, Urbana, IL 61801.

|| University of Michigan.

⊥ Academy of Sciences of the Czech Republic.

[1] Abbreviations: Bet, betaine; BHMT, betaine−homocysteine *S*-methyltransferase; CBHcy, S(δ-carboxybutyl)-L-homocysteine; DMG, dimethylglycine; Hcy, homocysteine; IF, intrinsic tryptophan fluorescence; Met, methionine; WT, wild type.

10.1021/bi049821x CCC: $27.50
Published on Web 04/16/2004

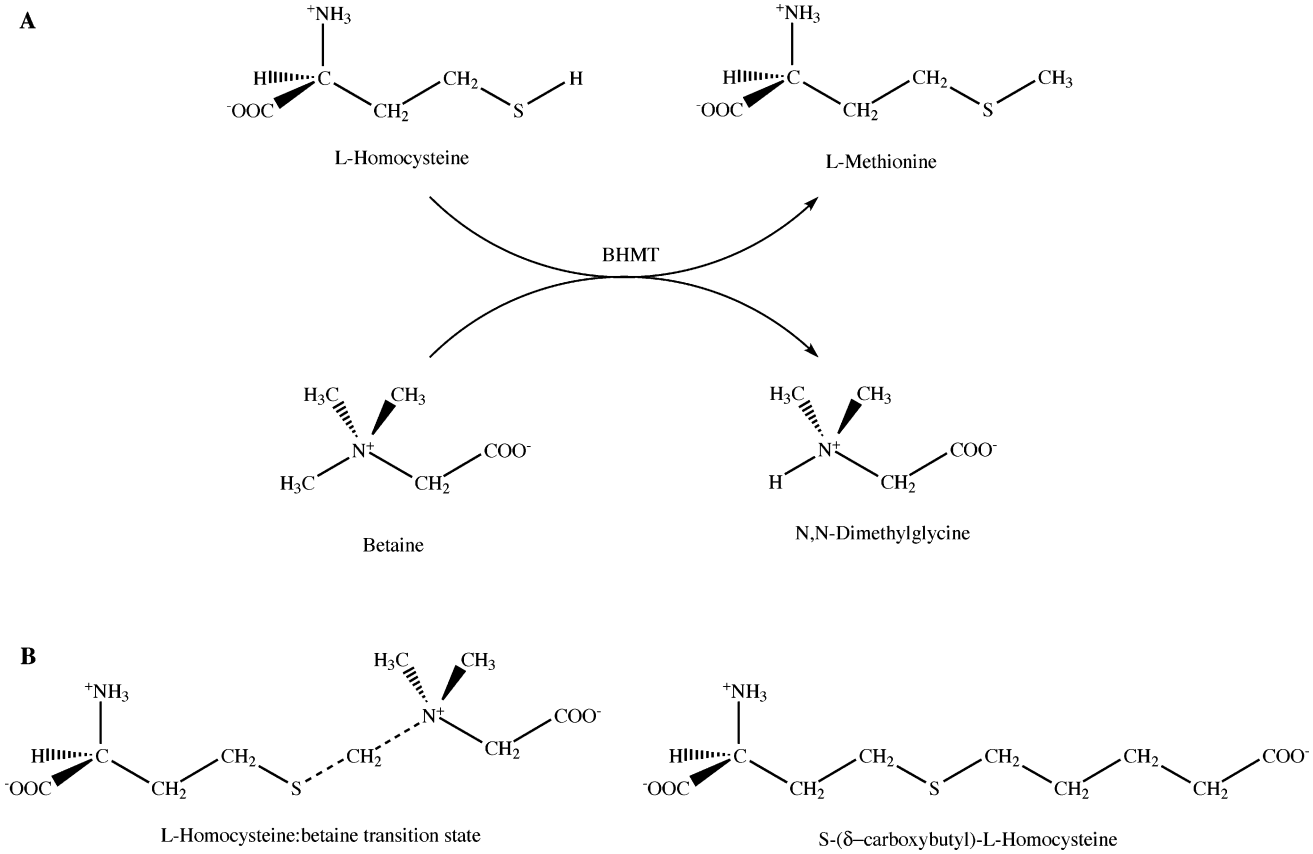

FIGURE 1: BHMT-catalyzed reaction. (A) Reaction shown with substrate and product structures. (B) Structure of the transition state and bisubstrate mimic, *S*-(*δ*-carboxybutyl)-L-homocysteine (CBHcy).

clearly demonstrated for BHMT or any member of the Hcy methyltransferase family.

Two X-ray structures of human BHMT have been determined (*1*), one depleted of zinc and the other zinc-replete with CBHcy bound. Enzyme crystallized in the absence of substrates loses zinc and is oxidized, with two of the three Cys residues that bind zinc connected by a disulfide bond. The CBHcy complex was obtained from these crystals by reconstituting the active site with zinc in the presence of DTT and the bisubstrate analogue. In both of the structures, BHMT is a dimer of dimers composed of four identical subunits (*1*, *11*), with very extensive and intricate interactions between the chains constituting each of the dimers. Each individual chain is folded into a $(\beta/\alpha)_8$ barrel in which the active site is assembled by distortions of the β-strands of the barrel. Following the barrel is a dimerization arm that wraps around the opposing chain of the dimer. The binding sites for Hcy and Bet can be inferred from the structure where the active site contains CBHcy (*1*). This structure identifies several conserved residues at the Hcy binding site that participate in substrate binding. In particular, Glu159, an invariant residue among homocysteine *S*-methyltransferases, hydrogen-bonds to the amino nitrogen in the L-Hcy moiety of CBHcy. The interactions of the carboxybutyl moiety of CBHcy identify residues that form the Bet binding site. The nonpolar butyl chain of CBHcy is surrounded by a ring of aromatic residues including Trp44, Tyr77, and Tyr160, which are expected to participate in the binding of Bet. In particular, the crystal structure predicts that the carboxyl group of Bet hydrogen-bonds to Trp44 and Tyr77.

In this paper it is shown that the binding of substrate, product, or CBHcy induces changes in the intrinsic tryptophan fluorescence (IF) of the enzyme and that quantification of these changes can be used to assess the affinity of the wild type (WT) and mutant proteins for these ligands. We use site-directed mutagenesis to examine the roles of Trp44, Tyr77, Glu159, and Tyr160 in BHMT function. Using the IF properties of BHMT, we have been able to demonstrate clearly that catalysis follows an ordered bi-bi mechanism and that Bet binding affinity is dependent on formation of the BHMT−Hcy complex. Scanning Trp mutagenesis, combined with IF measurements, has also provided a useful tool for assessing structural changes associated with the binding of substrates.

EXPERIMENTAL PROCEDURES

Materials. Oligonucleotide primers were made by IDT DNA Technologies (Coralville, IA). Bet, DMG, L- and DL-Hcy thiolactone, and L-Met were obtained from Sigma (St. Louis, MO). CBHcy was synthesized by one of the authors (J.J.). [*methyl*-^{14}C]-Bet was obtained from Moravek (Brea, CA). L- or DL-Hcy solutions (100 mM) were prepared fresh for each experiment. In brief, a thiolactone derivative (15.4 mg) was dissolved in 400 μL of 2 N sodium hydroxide, and after 5 m at room temperature, the solution was neutralized with 600 μL of a saturated monopotassium phosphate solution.

Human BHMT Protein Engineering, Expression, and Purification. The W44A, Y77F, E159Q, Y160F, W169F, W279F, W331F, W342F, W352F, and W373F mutants were constructed by use of the primers listed in Table 1 and the

Table 1: Oligonucleotide Primers for Site-Directed Mutagenesis

mutants	sequences of mutagenic primers[a]
W44A	5′-GGGGCTACGTAAAGGCAGGACCC**GCG**ACTCCTGAAGCTGCTGTG-3′
Y77F	5′-GTCATGCAGACCTTCACCTTC**TTT**GCGAGTGAAGACAAGCTGGAG-3′
E159Q	5′-GTGGACTTCTTGATTGCA**CAG**TATTTTGAACACGTTGAAGAA-3′
Y160F	5′-GACTTCTTGATTGCAGAG**TTT**TTTGAACACGTTGAAGAAGCTGTG-3′
W169F	5′-GAACACGTTGAAGAAGCTGTG**TTC**GCAGTTGAAACCTTGATAGCA-3′
W279F	5′-GAACCCAGAGTTGCCACCAGA**TTC**GATATTCAAAAATACGCCAGA-3′
W331F	5′-GCTTCAGAAAAACATGGCAGC**TTC**GGAAGTGGTTTGGACATGCAC-3′
W342F	5′-TTGGCAATGCACACCAAACCC**TTC**GTTAGAGCAAGGGCCAGGAAG-3′
W352F	5′-GCAAGGGCCAGGAAGGAATAC**TTC**GAGAATCTTCGGATAGCC -3′
W373F	5′-TCAATGTCAAAGCCAGATGGC**TTC**GGAGTGACCAAAGGAACAGCC-3′

[a] A pair of complementary primers was used to create each mutant, but only the sequence of the sense strand is shown. Changes in the sequences are shown in boldface type.

pTBY4-BHMT plasmid (*4*) as template, in combination with a Quikchange mutagenesis kit from Stratagene (La Jolla, CA). All plasmid inserts were sequenced at the University of Illinois' Biotechnology Center. Plasmid with either the WT BHMT cDNA or one of the above cited mutants were transformed into *Escherichia coli* BL21(DE3) cells. Expression and purification was carried out by use of the IMPACT-T7 expression and purification system (New England Biolabs) as previously described (*4*). Protein purity was analyzed by SDS−PAGE, and protein concentrations were determined by a Coomassie dye-binding assay (Bio- Rad Laboratories, Hercules CA) with bovine serum albumin as standard. The secondary structures of all mutants were analyzed by circular dichroism to ensure that the mutations did not affect gross secondary structure.

Fluorescence Measurements. Fluorescence emission spectra were obtained from BHMT kept in buffer containing 20 mM Tris (pH 7.5) and 5 mM 2-mercaptoethanol. Spectra were measured at 23 °C on a Fluoromax-3 spectrofluorometer from Jobin Ybon-Horiba (Edison, NJ). Excitation and emission slit widths of 4 nm were used with a cell having a 1 mm path length. The samples were excited at 295 nm to avoid Tyr fluorescence, and emission was scanned from 305 to 405 nm. Spectra were obtained from the WT and mutant proteins in the absence or presence of substrate and/or product or CBHcy. Only the L-forms of Hcy and Met were used. Spectra of enzyme-free solutions containing the corresponding concentration of ligand(s) were used as blanks for all experiments. Spectra were corrected by use of the software correction file (mcorrect) provided by the manufacturer.

Measurement of Ligand Binding by Changes in Steady-State IF. Changes in the steady-state IF intensity of BHMT when one substrate or product was held constant at saturating levels while the other was varied were used to calculate the ternary dissociation constant (K_d) of the varied substrate or product. The K_d for the BHMT−CBHcy binary complex also was calculated by measuring the incremental change in IF intensity following the addition of increasing concentrations of this inhibitor. For the above experiments, the change of emission intensity at 338 nm was quantified following excitation at 295 nm. The changes in the fluorescence emission maximum (λ_{max}) of BHMT following exposure to varying concentrations of Hcy or Met were used to calculate the K_d for the BHMT−Hcy and BHMT−Met binary complexes. In all cases the changes in normalized IF intensity values ($\Delta F' = F' - F_0'$), or normalized increments in λ_{max} ($\Delta\lambda_{max}' = \lambda_{max}' - \lambda_{max0}'$), were calculated by subtracting the normalized value obtained in the absence of ligand from the normalized value obtained at the different ligand concentrations. According to Eftink (*12*), the normalized values of ligand concentration versus $\Delta F'$, or ligand concentration versus increment in $\Delta\lambda_{max}'$, were fit to the quadratic equation shown in eq 1 (*13*), which assumes one binding site per macromolecule, as is the case for the BHMT monomer:

$$[EL] = {}^1/_2\{[E] + [L] + K_d - ([E] + [L] + K_d)^2 - 4[E][L]/2\} \quad (1)$$

where [E] is the concentration of enzyme, [L] is the concentration of the varied ligand (inhibitor, substrate, or product), and [EL] is the concentration of enzyme−ligand complex. [E] in the steady-state experiments described herein was 0.2 μM for studies with CBHcy and 1 μM for studies with substrate(s) and/or product(s) and is based on the concentration of active sites; that is, the concentration of the monomeric subunit. The total amount of [EL] formed was calculated from the normalized steady-state increments in IF intensity ($\Delta F'$) or λ_{max} ($\Delta\lambda_{max}'$). Curve-fitting was performed with Kaleidagraph software (Sinergy Software, Reading, PA)

BHMT Activity and Enzyme Kinetics. BHMT activity was measured as described by Garrow (*14*). The standard assay contains 5 mM DL-Hcy and 2 mM Bet (0.1 μCi). To determine the K_m for Bet, initial rate data were obtained with saturating levels of DL-Hcy (5 mM) while the concentration of Bet was varied from 0.25 to 40 mM (0.5 μCi). To determine the apparent K_m for L-Hcy, initial rate data were obtained with subsaturating levels of Bet (250 μM, 0.5 μCi) while the concentration of L-Hcy was varied from 1 μM to 1 mM. The K_m and V_{max} constants were estimated by fitting initial rate data according to the method of Hanes (*15*).

RESULTS

Changes in the IF of BHMT upon Ligand Binding. We have characterized the steady-state IF signal of BHMT in the absence and presence of substrate, product, and CBHcy following excitation at 295 nm. In the absence of ligands, the fluorescence emission spectrum of BHMT displays a λ_{max} of 334 nm (Figure 2A), blue-shifted compared to free Trp ($\lambda_{max} \approx 350$ nm).

Incubation of the enzyme with an individual substrate or product causes differing effects on the IF signal, including changes in its λ_{max} and emission intensity. Addition of either Hcy or Met induces a concentration-dependent red shift in

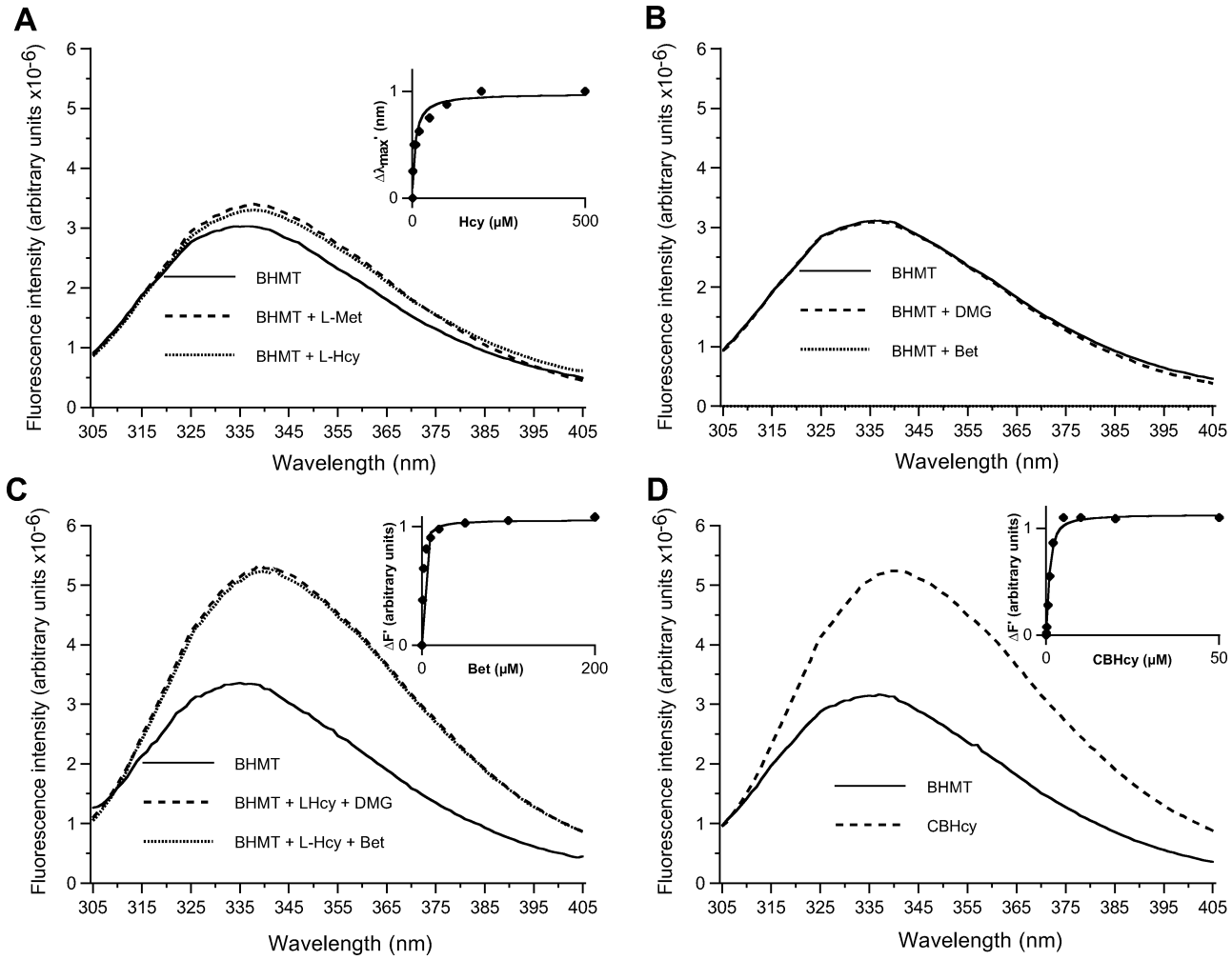

FIGURE 2: Fluorescence emission spectra of substrate-free WT BHMT and changes induced upon ligand binding. Spectra were obtained as described under Experimental Procedures. Protein solutions contained 20 mM Tris (pH 7.5) and 5 mM 2-mercaptoethanol. An excitation wavelength of 295 nm was used, and emission was scanned from 305 to 405 nm. Steady-state fluorescence intensity was recorded with a λ_{ex} of 295 nm and a λ_{em} of 338 nm. **(**A**)** Emission spectra of WT BHMT (1 μM) (solid line) and WT BHMT after incubation with saturating concentrations of Met (1 mM) (dashed line) or Hcy (1 mM) (dotted line). Inset: Concentration-dependent shift of λ_{max}' with increasing concentrations of Hcy (1 μM enzyme). The plot shows normalized values of $\Delta\lambda_{max}'$ vs [Hcy] fit to eq 1. A similar $\Delta\lambda_{max}'$ vs [Met] relationship was observed (not shown). **(**B**)** Emission spectra of WT BHMT (1 μM) (solid line) and WT BHMT after incubation with DMG (1 mM; dashed line) or Bet (1 mM; dotted line). **(**C**)** Emission spectra of WT BHMT (1 μM) (solid line) and WT-BHMT after incubation with saturating concentrations of either Hcy and DMG (1 mM each; dashed line) or Hcy and Bet (1 mM each; dotted line). Inset: Concentration-dependent steady-state fluorescence intensity of WT BHMT (1 μM) exposed to saturating concentrations of Hcy (1 mM) and increasing concentrations of Bet. The plot shows normalized values of $\Delta F'$ vs [Bet] that were fit to eq 1. **(**D**)** Emission spectra of WT BHMT (1 μM) (solid line) and WT BHMT after incubation with a saturating concentration of CBHcy (100 μM; dashed line). Inset: Concentration-dependent steady-state fluorescence intensity of WT BHMT (0.2 μM) exposed to increasing concentrations of CBHcy. The plot shows normalized values of $\Delta F'$ vs [CBHcy] fit to eq 1.

the λ_{max} of the enzyme (example in Figure 2A, inset). At saturating levels of Hcy or Met the shift in λ_{max} is 4 nm, and it is accompanied by a very small increase in the intensity of the signal (Figure 2A). On the basis of the work of Callis (*16*), the observed shift in λ_{max} toward longer wavelengths when BHMT binds Hcy or Met suggests that one or more Trp residues relocate to a more polar environment. No change in either λ_{max} or fluorescence intensity was observed when BHMT was incubated with DMG or Bet (Figure 2B), suggesting that either these ligands have no affinity for the free enzyme or the binding of these ligands does not produce a measurable change in the IF signal.

A different IF signal for BHMT is observed when the enzyme forms a complex with Hcy and Bet, Hcy and DMG, or CBHcy. The addition of saturating concentrations of these ligands (1 mM Hcy with 1 mM Bet or DMG, or 100 μM CBHcy) causes a 58% increase in the IF intensity of the enzyme and an 8 nm red shift (λ_{max} = 342 nm) (Figure 2C,D). The observed increase in the IF intensity of BHMT upon the addition of Hcy and Bet, or Hcy and DMG, is concentration-dependent when Hcy is held at saturating concentrations (1 mM Hcy) and the concentration of Bet or DMG is varied (example in Figure 2C, inset). Similarly, the IF intensity is also dependent on the concentration of Hcy if Bet or DMG are held at saturating levels (1 mM). Graded additions of CBHcy also cause a concentration-dependent increase in IF intensity (Figure 2D, inset). In contrast to the additional 4 nm shift in λ_{max} and the large increase in IF intensity when either Bet or DMG is added to the BHMT−Hcy complex, no further change in the IF signal of BHMT is observed when high levels of Bet or DMG are added to the BHMT−Met complex.

Scheme 1: Kinetic Mechanism of the BHMT Reaction[a]

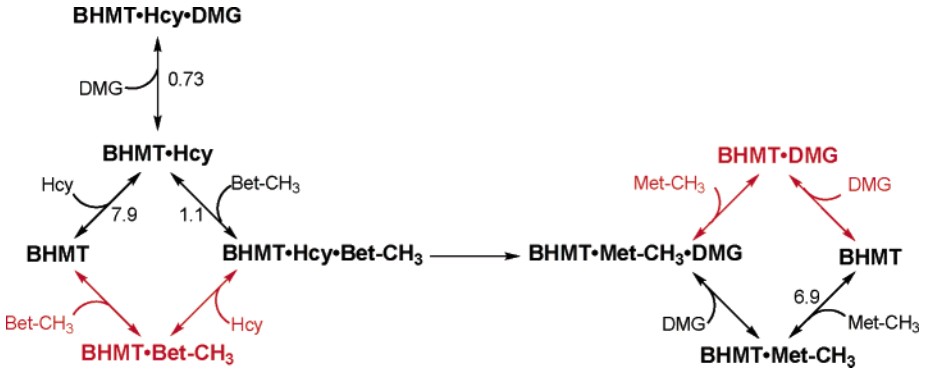

[a] The ordered bi-bi reaction sequence of substrate addition and product release is shown in black, and the unused paths are shown in red. The K_d values for the various complexes are shown, including the abortive ternary complex BHMT−Hcy−DMG.

Table 2: Dissociation Constants for Substrates, Products, and CBHcy for WT BHMT

substrate, product, or inhibitor	dissociation constant (K_d)	K_d value (μM)
Hcy	$K_{d\,Hcy}$[a]	7.9, 11, 8.6
Bet	$K_{d\,Bet}$[b]	1.1
DMG	$K_{d\,DMG}$[b]	0.73
Met	$K_{d\,Met}$[c]	6.9
CBHcy	$K_{d\,CBHcy}$[d]	0.28

[a] Dissociation constants for L-Hcy were calculated by three different methods: for the first value shown, K_d was calculated by measuring the shift in λ_{max} undergone by BHMT incubated with increasing concentrations of Hcy (binary complex); for the second value shown, K_d was calculated by measuring changes in IF intensity at saturating concentrations of Bet (1 mM) and increasing concentrations of Hcy (ternary complex); and for the third value shown, K_d was calculated by measuring changes in IF intensity at saturating concentrations of DMG (1 mM) and increasing concentrations of Hcy (ternary complex). [b] Dissociation constants for Bet and DMG were calculated by measuring changes in IF intensity at saturating concentrations of L-Hcy (1 mM) and increasing concentrations of either Bet or DMG (ternary complexes). [c] The dissociation constant for L-Met was calculated by measuring the shift in λ_{max} undergone by BHMT incubated with increasing concentrations of Met (binary complex). [d] The dissociation constant for CBHcy was calculated by measuring changes in steady-state fluorescence intensity at increasing concentrations of CBHcy (binary complex).

Dissociation Constants of Ligands for BHMT Can Be Determined from IF Changes. By using the Hcy- and Met-dependent shift of λ_{max} when these ligands bind to BHMT, the dissociation constants ($K_{d\,Hcy}$ and $K_{d\,Met}$) of these binary complexes were determined to be 7.9 and 6.9 μM, respectively (Table 2). By quantifying changes in the IF intensity that accompany binding of the second substrate, K_ds were determined for Bet or DMG binding to the BHMT−Hcy complex. The $K_{d\,Bet}$ and $K_{d\,DMG}$ values for formation of the corresponding ternary complexes are 1.1 and 0.73 μM, respectively. The K_d for Hcy also was measured by changes in IF intensity upon Hcy binding in the presence of saturating concentrations (1 mM) of Bet or DMG (Table 2). The $K_{d\,Hcy}$ values were 11 and 8.6 μM, respectively, approximately the same as the K_d for formation of the binary complex of BHMT with Hcy. The agreement between these measured K_ds is consistent with the ordered mechanism depicted in Scheme 1. The K_d for the BHMT−CBHcy binary complex (0.28 μM) was similarly determined from the increments in IF intensity (Table 2).

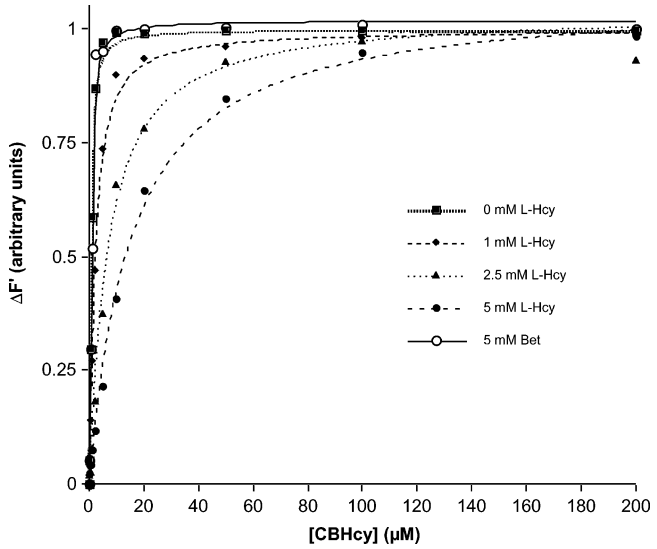

FIGURE 3: Ability of Hcy or Bet to compete with CBHcy for binding to WT BHMT. Steady-state fluorescence intensity was measured with a λ_{ex} of 295 nm and a λ_{em} of 338 nm. Spectra were obtained from WT BHMT (0.2 μM) in solutions containing 20 mM Tris (pH 7.5) and 5 mM 2-mercaptoethanol in the absence or presence of Hcy (1, 2.5, and 5 mM) or Bet (5 mM), and the specified concentrations of CBHcy. Substrates were added prior to CBHcy. Normalized $\Delta F'$ values were plotted vs the concentration of CBHcy.

BHMT Follows an Ordered Bi-Bi Mechanism. The total change in the IF signature of BHMT when both binding sites are occupied can be separated into two distinct phases: an initial 4-nm red shift in λ_{max} associated with the occupation of the Hcy binding site and a second (additional) 4-nm red shift and enhanced IF intensity when the Bet binding site is occupied by Bet or DMG. These changes happen in concert when the bisubstrate analogue (CBHcy) binds to the enzyme. To determine whether Bet or DMG could bind to BHMT in the absence of Hcy, we monitored the ability of Bet, DMG, and Hcy to compete with CBHcy for the active site by steady-state fluorescence. $K_{d\,CBHcy}$ in the absence of Hcy is 0.28 μM (Table 2). However, in the presence of 1, 2.5, or 5 mM Hcy the apparent $K_{d\,CBHcy}$ increases to 1.6, 6.3, or 14.5 μM, respectively (Figure 3). In contrast, in the presence of 5 mM Bet (Figure 3) or DMG (not shown), the K_d measured for CBHcy is not affected. Failure of Bet or DMG to compete with CBHcy confirms that Bet and DMG have no detectable affinity for BHMT unless a ligand already occupies the Hcy

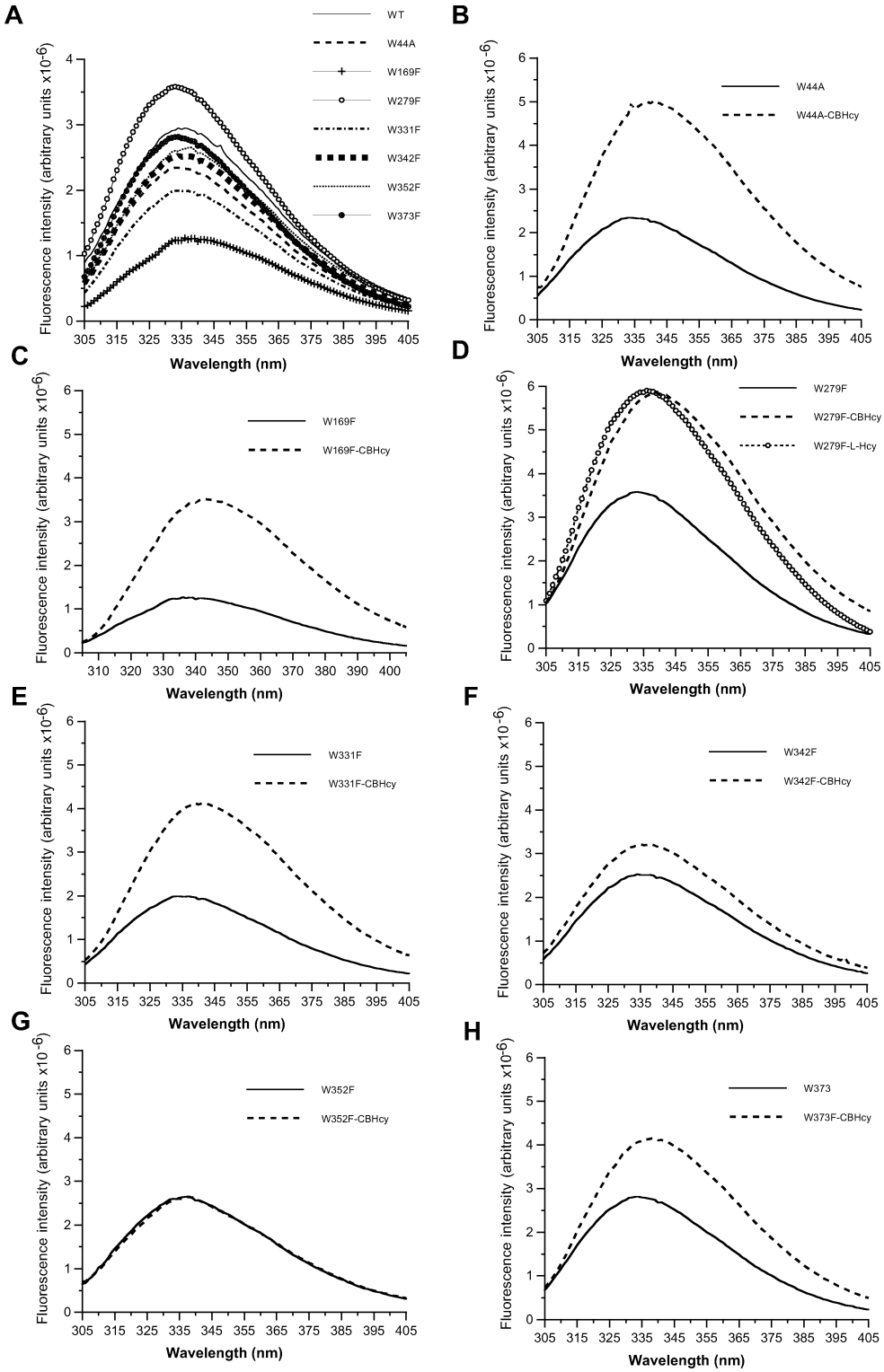

FIGURE 4: Changes in the fluorescence emission spectra of WT BHMT and derived Trp mutants upon binding CBHcy. Spectra were obtained as described under Experimental Procedures. Protein solutions (1 μM) contained 20 mM Tris (pH 7.5) and 5 mM 2-mercaptoethanol. An excitation wavelength of 295 nm was used, and emission was scanned from 305 to 405 nm. (A) Emission spectra of WT BHMT and the Trp mutants in the absence of ligand. (B, C, E−H) Emission spectra of the Trp mutants before and after the addition of saturating concentrations of CBHcy (100 μM). (D) Emission spectrum of substrate-free W279F, and following the addition of saturating concentrations of Hcy (1 mM) or CBHcy (100 μM).

binding site. As mentioned earlier, there is no additional shift in λ_{max} or IF intensity when the BHMT−Met complex is presented with high concentrations of DMG (Figure 2B). Taken together, these results demonstrate that BHMT follows an ordered bi-bi mechanism in which Hcy is the first substrate bound and Met is the last product released.

Systematic Mutagenesis of All Tryptophan Residues in BHMT. BHMT contains seven Trp residues and the crystal structure shows that Trp44 is part of the active site of BHMT, forming a hydrogen bond to the carboxylate group of CBHcy (*1*). To determine whether the observed IF changes accompanying ligand binding are due to changes in the environment

Table 3: Shift in λ_{max} of WT BHMT and Trp Mutants upon Incubation with Saturating Concentrations of Hcy or CBHcy[a]

		λ_{max} value (nm)	
enzyme	enzyme alone	enzyme + Hcy	enzyme + CBHcy
WT	334	338	342
W44A	334	338	342
W169F	338	338	343
W279F	334	338	342
W331F	334	338	342
W342F	334	334	336
W352F	336	337	338
W373F	334	334	338

[a] Values were obtained from the emission spectrum of WT and mutant enzymes as described under Experimental Procedures. Emission spectra were obtained with an excitation wavelength of 295 nm, and emission was scanned from 305 to 405 nm (23 °C). Measurements were taken every 1 nm.

Table 4: Kinetic Parameters for BHMT and Active-Site Mutants[a]

enzyme	V_{max}[b] (units/mg)	$K_{m\ Bet}$[b] (mM)	V_{max}/K_m[b] (relative)	V_{max}[c] (units/mg)	$K_{m\ Hcy}$[c] (μM)	V_{max}/K_m[c] (relative)
wild type	11 000	1.7	100	1300	9.7	100
W44A	11 000	7.5	23	nd	nd	nd
Y160F	12 000	>30	<6.2	nd	nd	nd
Y77F[d]	nd[d]	nd	nd	nd	nd	nd
E159Q	nd	nd	nd	2000	270	5.7

[a] Initial rate kinetics were performed as described under Experimental Procedures. A unit of activity is defined as 1 nmol of product formed per hour. [b] Bet was varied (0.25−40 mM) while the concentration of D,L-Hcy was held constant at saturating levels (5 mM). V_{max}/K_m values are relative to that obtained for the WT enzyme (equals 100). [c] L-Hcy was varied (1−1000 μM) while the concentration of Bet was held constant at subsaturating levels (250 μM); therefore, kinetic parameters obtained for Hcy are apparent. V_{max}/K_m values are relative to that obtained for the WT enzyme (equals 100). [d] Y77F was discovered to be inactive. [e] Not determined.

of Trp44 or other Trp residues, we measured the IF signal of the following mutants: W44A, W169F, W279F, W331F, W342F, W352F, and W373F. The IF spectra of these mutants in the absence and presence of Hcy, Met, Hcy and DMG, and CBHcy were compared to the corresponding WT BHMT spectra. Notably, the activities of these Trp mutants in the standard assay were not significantly different from the WT enzyme, except for W44A, which had only 33% of WT activity and will be discussed below.

The changes in the IF signal of ligand-free BHMT that result from the replacement of each Trp are shown in Figure 4A and in Table 3. The emission intensity of W44A, W342F, W352F, and W373F, although a little lower than that of the WT enzyme, is not significantly altered. The IF intensities of W169F and W331F are clearly lower than the WT enzyme, indicating that these residues make important contributions to the emission spectra of ligand-free WT BHMT (Figure 4A). The emission of W279F is higher than that of the WT enzyme, suggesting that W279 may be quenching the fluorescence of other Trp residues in the WT enzyme (see Discussion).

The effects of each mutation on the IF shifts induced by Hcy binding are shown in Table 3. In the presence of saturating concentrations of Hcy or Met (not shown), W44A, W279F, and W331F display the same 4-nm shift in λ_{max} as the WT enzyme. No shift in λ_{max} was observed when W169F, W342F, or W373F was incubated with high concentrations of Hcy or Met, and only a small shift ($\Delta\lambda_{max} \sim 1$ nm) was observed for W352F. The simplest interpretation of these data is that binding in the Hcy site induces structural changes that are reported by Trps 169, 342, 352, and 373.

The effects of each mutation on the IF shifts induced by CBHcy binding are shown in Figure 4B−H and Table 3. Compared to the enzymes in the presence of saturating levels of Hcy, incubation of W44A, W169F, W279F, W331F, and W373F with saturating concentrations of the bisubstrate analogue CBHcy (Table 3) or the Hcy/DMG pair (not shown) leads to an additional 4−5-nm shift in λ_{max}, like that observed for the WT enzyme. A smaller shift was observed with W342F and W352F ($\Delta\lambda_{max} \sim 1-2$ nm). No increase in IF intensity was observed with W352F (Figure 4G), and only a small increase was observed for W342F (Figure 4F). Besides W373F, which showed an intermediate increase in IF intensity upon CBHcy binding (Figure 4H), the remainder of the mutants behaved like the WT enzyme (Figure 4B−E, Table 3). These results indicate that Trp342 and Trp352 have a critical role in reporting the structural changes that accompany the occupation of the Bet binding site.

The spectrum of the W279F−Hcy complex is unique. In the presence of 1 mM Hcy this mutant enzyme displays a dramatic increase in IF intensity (Figure 4D) in addition to the normal 4-nm red shift (Table 3). In WT and in other mutants, this large increase in IF intensity is observed only in the presence of saturating concentrations of CBHcy (Figure 2D), or with Hcy and Bet or Hcy and DMG (Figure 2C). Trp279 is one of three Trps that are closely clustered in the crystal structure (Figure 8 and Discussion).

Analysis of the Residues Involved in Bet Binding. To determine if Trp44, Tyr 77, and Tyr160 are involved in the binding of Bet, we performed site-directed mutagenesis and replaced Tyr77 and Tyr160 with Phe (Y77F and Y160F). We then assayed the ability of W44A, Y77F, and Y160F to bind Hcy, DMG, or CBHcy and calculated the dissociation constants for these ligands by the IF methods described above. Although the turnover of BHMT is very slow (9 min^{-1} at 37 °C), and the steady-state fluorescence measurements were performed at 23 °C within 10 s, we avoided any complications resulting from product formation by not using Bet in these experiments.

As indicated above (Figure 4B), W44A has an IF signal in the absence and presence of CBHcy (saturating concentrations) similar to that of the WT protein. However, this mutant has only 33% of the activity of the WT enzyme when measured by the standard assay. W44A has a $K_{d\ Hcy}$ of 8.7 μM, which is similar to that of the WT enzyme. However, the ternary $K_{d\ DMG}$ for W44A is 13 μM, about 8 times higher than that of the WT enzyme (Table 2). Consistent with a defect in the Bet binding site, the $K_{d\ CBHcy}$ for W44A is 2.6 μM, almost 10 times higher than WT enzyme (Table 2). These results indicate that Trp44 is important for the binding of DMG and Bet, as implied by the crystal structure of the enzyme complexed with CBHcy (17). W44A also was characterized by initial rate kinetics with saturating levels of Hcy and varying levels of Bet. The K_m and V_{max} values for WT and W44A are shown in Table 4. The K_m for Bet is more than 4-fold larger for W44A than for WT enzyme, while the V_{max} is unaffected. The net effect is that the catalytic efficiency ($V_{max}/K_{m\ Bet}$) of W44A is about 23% of the WT enzyme.

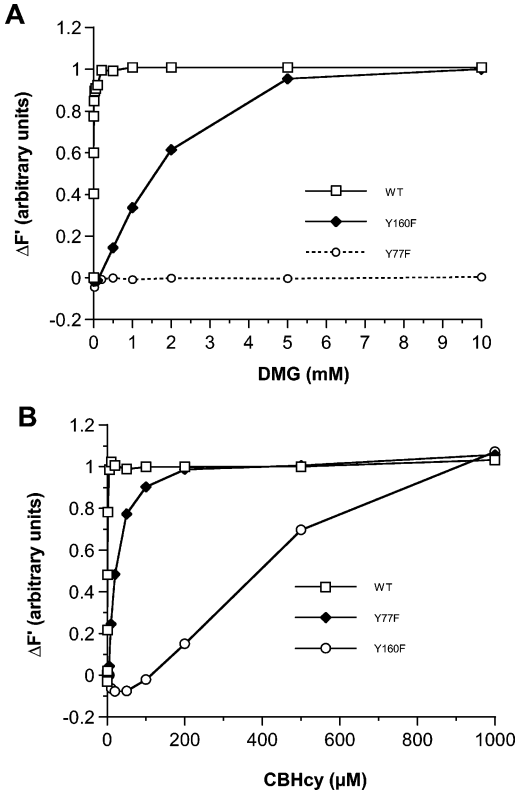

FIGURE 5: Ability of Y77F and Y160F to bind DMG or CBHcy. Protein solutions contained 20 mM Tris (pH 7.5) and 5 mM 2-mercaptoethanol. **(**A**)** Steady-state fluorescence intensity of WT-BHMT (1 μM), Y77F (1 μM), and Y160F (1 μM) were saturated with Hcy (1 mM) and then presented with increasing concentrations of DMG. Normalized $\Delta F'$ values were plotted vs the concentration of DMG. **(**B**)** Concentration-dependent changes in steady-state fluorescence intensity of WT BHMT (0.2 μM), Y77F (0.2 μM), and Y160F (0.2 μM) upon binding CBHcy. Normalized $\Delta F'$ values were plotted vs the concentration of CBHcy.

The IF signals of Y160F in the absence or presence of saturating levels of CBHcy are similar to the IF signals observed for the WT enzyme (not shown). The addition of saturating concentrations of Hcy and DMG to the Y160F enzyme induces changes in the IF intensity and a shift in λ_{max} (8 nm) that are identical to those observed for the WT enzyme (not shown). However, the concentrations of DMG required to attain the maximum changes in fluorescence are much higher than required by the WT enzyme (Figure 5A). It also takes much higher concentrations of CBHcy to saturate Y160F with this ligand (Figure 5B). No changes in the K_d for Hcy are observed for Y160F when determined using saturating levels of DMG and increasing concentrations of Hcy, suggesting that Tyr160 is only involved in the binding of Bet and DMG. In addition, initial rate kinetics using saturating levels of Hcy and varying levels of Bet show that the K_m for Bet for Y160F is more than 10-fold higher than that measured for the WT enzyme, while V_{max} is not affected (Table 4). The Y160F mutant has a catalytic efficiency ($V_{max}/K_{m\,Bet}$) that is only about 5% that of the WT enzyme.

The IF signals of Y77F in the absence or presence of saturating levels of CBHcy are similar to the IF signals observed for the WT enzyme (not shown). We were surprised to find that incubation of Y77F with high concentrations of Hcy (up to 5 mM) did not induce the 4-nm shift in λ_{max} observed for the WT enzyme (not shown), nor are there any changes in the IF intensity of this mutant when it is incubated with saturating levels of Hcy and DMG (up to 5 mM each) (Figure 5A). These observations are consistent with our finding that Y77F is devoid of activity when measured by the standard assay. It is interesting that Y77F does display normal changes in its IF signal upon the addition of saturating concentrations of CBHcy (Figure 5B). Although relatively high concentrations (>20 μM; $K_{d\,CBHcy}$ = 28 μM) are required to elicit this response, the binding of CBHcy to this mutant indicates that the bisubstrate analogue can force the enzyme to adopt its final catalytic conformation without the aid of Tyr77.

Role of E159 in the Binding of Hcy. To study the functional role of Glu159, we changed this residue to Gln (E159Q). Changes in the fluorescence emission spectrum of BHMT have been used to analyze the ability of E159Q to bind Hcy, DMG, and CBHcy, and steady-state activities were assayed.

The IF spectrum of ligand-free E159Q is similar to the WT enzyme with respect to λ_{max} and total IF intensity (not shown). We tested the affinity of this mutant for Hcy by incubating E159Q with saturating concentrations of DMG (1 mM) while the concentration of Hcy was varied (Figure 6A). Under these conditions, higher Hcy concentrations are required to induce changes in the IF intensity of E159Q than the WT enzyme. The $K_{d\,Hcy}$ for E159Q is 1.2 mM, approximately 400-fold higher than the WT enzyme. However, the K_d for DMG binding to the BHMT−Hcy complex remained unchanged (not shown). E159Q exhibits a K_d for CBHcy of 2.6 μM, a 6-fold increase compared to WT enzyme (Figure 6B). Initial rate kinetics of E159Q toward Hcy was assessed with subsaturating levels of Bet (250 μM) and varying concentrations of Hcy. The apparent K_m and V_{max} values were calculated and are shown in Table 4. The apparent K_m for Hcy is 28-fold higher for E159Q than that measured for the WT enzyme (Table 4). In addition, this mutant displays a higher apparent V_{max}, which indicates that this mutation somehow affects catalytic rate. The E159Q mutant has a catalytic efficiency (V_{max}/K_m) that is only about 6% that of the WT enzyme.

DISCUSSION

Mechanistic Features of the BHMT Reaction. Changes in the fluorescence emission spectrum of BHMT that arise following the addition of substrates, products, or CBHcy have been exploited to measure binding constants that support the ordered bi-bi mechanism presented in Scheme 1. This paper is the first to report measurements of the dissociation constants of BHMT for Hcy, Bet, Met, DMG, and CBHcy.

Previous studies described DMG as a potent inhibitor of human (*17*, *18*), porcine (*19*), and rodent (*9*) BHMT, although a K_i for DMG has never been reported. The present studies support the conclusion that DMG is a potent inhibitor of BHMT and demonstrate that DMG inhibition is caused by the formation of an abortive BHMT−Hcy−DMG complex. The dissociation constant of DMG for the BHMT−Hcy complex is low (0.73 μM), indicating that the abortive complex can be formed at physiological concentrations of Hcy and DMG. These data support our earlier suggestion that flux through the BHMT reaction in patients with severe hyperhomocysteinemia (>100 μM) receiving oral Bet treatment is probably regulated in part by DMG concentra-

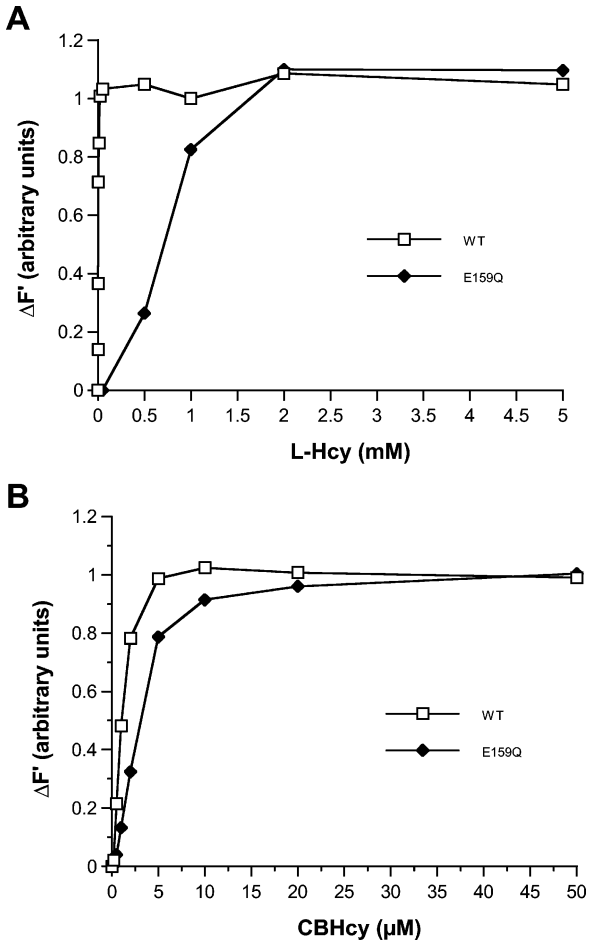

FIGURE 6: Effect of Hcy or CBHcy binding to E159Q on its steady-state fluorescence intensity. Protein solutions contained 20 mM Tris (pH 7.5) and 5 mM 2-mercaptoethanol. **(**A**)** Change in steady-state fluorescence intensity of WT BHMT(1 μM) and E159Q (1 μM) upon incubation with saturating concentrations of DMG (1 mM) prior to the addition of increasing concentrations of Hcy. Normalized $\Delta F'$ values were plotted vs the concentration of L-Hcy. **(**B**)** Change in steady-state fluorescence intensity of WT BHMT (0.2 μM) and E159Q (0.2 μM) upon incubation with increasing concentrations of CBHcy. Normalized $\Delta F'$ values were plotted vs the concentration of CBHcy.

tions (*14*). In that report it was noted that patients undergoing Bet treatment still have moderate hyperhomocysteinemia (30−50 μM) and have dramatic increases in plasma Bet and DMG, the latter being greater than 30-fold above normal (up to 250 μM). Our studies support the idea that the inability to catabolize or excrete the excess DMG produced from Bet loading to prevent its accumulation precludes further reductions in plasma Hcy via the BHMT-catalyzed reaction because of the formation of the BHMT−Hcy−DMG abortive complex. A more recent study in patients with chronic renal failure showed that their plasma Hcy levels were correlated positively with plasma DMG (*20*). These clinical data support the idea that the abortive, ternary BHMT−Hcy−DMG complex has physiological relevance.

We do not find any changes in fluorescence after the addition of Bet or DMG to enzyme incubated with Met, indicating that the binding of Bet or DMG to the BHMT−Met complex is very weak. It is not surprising that the BHMT−Met−Bet complex cannot form since the two methyl groups might overlap at the active site. The reason for weak binding of DMG to the BHMT−Met complex is not obvious. It may be that the electrostatic interaction between the negative thiolate of Hcy and the positive quaternary amine of Bet is the largest contribution to the binding energy for Bet; this interaction is lost in the product complex. This idea is consistent with the observations that Bet binds to the BHMT−Hcy complex with a K_d value of 1.1 μM (Table 2), whereas a Bet analogue in which the nitrogen atom has been replaced with carbon (3,3-dimethylbutyrate) is a weak competitive inhibitor of Bet binding with a K_i value of 450 μM (*17*). The fact that the BHMT−Met complex can be detected by fluorescence but the BHMT−Met−DMG complex cannot indicates that the equilibrium is displaced toward the form BHMT−Met (Scheme 1), validating the hypothesis that DMG is the first substrate to dissociate.

Mutagenesis of Active-Site Residues. The crystal structure of BHMT in complex with CBHcy identified Glu159, an invariant residue in the thiol/selenol methyltransferase family (Pfam 02574), as a hydrogen-bond acceptor for the amino group of Hcy. Mutation of Glu159 to Gln results in an enzyme with very low catalytic efficiency. Analysis of its capacity to bind Hcy shows that this mutant has decreased affinity for Hcy and CBHcy, while the affinity for Bet and DMG in the presence of saturating concentrations of Hcy remains unchanged. Additionally, initial rate kinetics reveal that although this mutant has a 50% higher $V_{max\ app}$, the $K_{m\ app}$ for Hcy is substantially higher than that for the WT enzyme. These results are similar to those obtained by González et al. (*21*), who showed that the E159G and E159K mutations in the rat enzyme increased the K_m for Hcy. However, these mutants also had significantly lower V_{max} values than the WT enzyme. Because these latter mutations introduce large changes in the shape and charge of the active site, it would be useful to know whether these substitutions provoked structural perturbations beyond the immediate vicinity of the side chain.

In the structure of the human enzyme, the carboxybutyl moiety of CBHcy serves as a surrogate for Bet and is encircled by a ring of aromatic residues including W44, Y77, and Y160. Trp44 and Tyr77 each form hydrogen bonds with oxygen atoms of the carboxylate moiety of CBHcy (*1*), while Tyr160 is packed against Tyr77. We used site-directed mutagenesis to examine the contributions of these residues to substrate binding and catalysis. Changing W44 to Ala and Y160 to Phe did not affect the ability of BHMT to bind Hcy, but DMG and CBHcy binding were impaired in these mutants (Figure 5). These enzymes displayed normal turnover rates but had significantly higher K_m values for Bet (Table 4). The ligand binding and kinetic properties of W44A and Y160F clearly show that W44 and Y160 are important determinants for Bet and DMG binding.

It was surprising to find that the Y77F mutant displays no activity in the standard BHMT assay. González et al. (*21*) reported that the Y77A mutant of the rat enzyme retained 7% of the activity measured for the WT enzyme. High concentrations of Hcy (up to 5 mM) or high concentrations of Hcy and Bet or Hcy and DMG fail to induce changes in the IF signal of the Y77F mutant, but high concentrations of CBHcy induce the normal large increase in IF intensity. However, the red shift in λ_{max} is smaller than normal and the K_d for this ligand increases 100-fold. The apparent involvement of Tyr77 in Hcy binding is curious because the crystal structure would suggest that this residue serves only

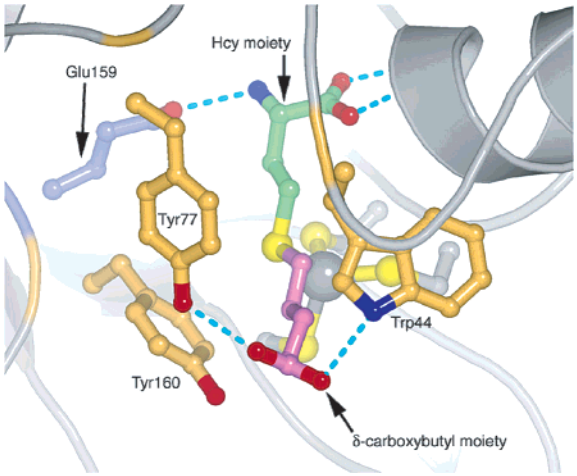

FIGURE 7: CBHcy and its interactions with BHMT. CBHcy is shown in the center of this figure, with the Hcy moiety in pale green and the δ-carboxybutyl moiety in lavender. The thioether of CBHcy is bound to the zinc cluster, with the zinc ion shown as a gray sphere. Hydrogen-bond interactions are depicted as cyan dots. The interactions of the bisubstrate analogue with the protein establish the binding sites for the two substrates, Hcy and Bet. Hcy is coordinated to the protein by its interaction with zinc, a hydrogen bond formed between the Hcy amino group and Glu159, and bidentate hydrogen bonds formed to the backbone amides of helix αB. The δ-carboxybutyl group of CBHcy, which mimics Bet, forms hydrogen bonds with Trp44 and Tyr77, with Tyr160 stacking against the long, aliphatic butyl group.

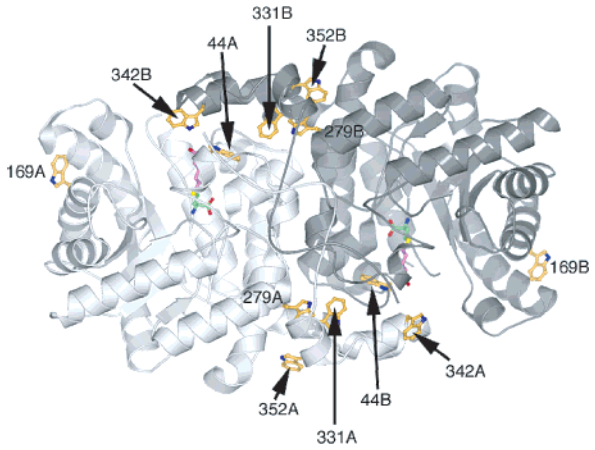

FIGURE 8: Dimer of BHMT with all tryptophan residues highlighted. This image is derived from the crystal structure of BHMT and is oriented so that the noncrystallographic 2-fold axis of symmetry is in the center of the molecule shown. Each tryptophan residue in the structure is labeled and shown in gold. The bound CBHcy ligand is shown for reference and is colored as in Figure 7.

as a binding determinant for the carboxyl moiety of the Bet mimic (Figure 7). It is possible that nonlocal structural perturbations are introduced by the Y77F mutation. The precise role of Y77 in substrate binding and catalysis requires further investigation.

Fluorescence Changes and Their Implications. Trp fluorescence has been widely used to characterize the binding of ligands to proteins. The fluorescence of the indole chromophore is highly sensitive to environment, making it a convenient choice for reporting protein conformational changes and ligand−protein interactions (*22*). However, it is difficult to assess the nature and magnitude of conformational changes from fluorescence measurements.

The fluorescence emission spectrum of BHMT reports contributions from all seven Trp residues in the protein (Figure 4A). The large number of Trp residues in BHMT complicates the interpretation of the spectral changes, and we therefore employed mutagenesis to determine the effect on the IF of removing individual reporter residues. Except for Trp373, the crystal structure provides information about the positions and environment of Trp residues that we can attempt to correlate with the effects of mutations on binding and fluorescence (Figure 8).

Site-directed mutagenesis confirms that the first shift in λ_{max} (from 334 to 338 nm), induced by Hcy or Met binding, and the second shift in λ_{max} (from 338 to 442 nm), induced by Bet or DMG binding and accompanied by an increase in IF intensity, are caused by two distinct structural changes. The mutants W169F and W373F do not undergo any changes in fluorescence upon the binding of Hcy, indicating that in WT BHMT these Trp residues report the structural changes associated with formation of the BHMT−Hcy complex. However, binding of Hcy and Bet, Hcy and DMG, or CBHcy to these mutants still elicits shifts in λ_{max} and a large increase in IF intensity, indicating that occupation of the Bet site is reported by different Trp residues.

Trp169 is near the surface of the protein, far from either active site of the dimer (Figure 8), surrounded by charged residues and held in place by two Glu side chains. The structures do not offer an explanation for the perturbation of the fluorescence of the W169F−Hcy complex. Similarly, there is no direct structural information to correlate Trp373 with the fluorescence changes, but Asp371, the last residue that is visible in the crystal structure, is close to Trp342 in the dimerization arm of the neighboring chain, and it is reasonable to assume that Trp373 is also near the dimerization arm of the neighboring chain. One of the most intriguing structural differences between the oxidized enzyme and the complex with CBHcy (zinc-replete) is a shift of the accessory helix αB that is involved in the binding of Hcy, but it is not clear how Trp169 and Trp373 might report the movement of helix αB.

W342 and W352 report the changes in IF intensity associated with binding of the carboxybutyl group of CBHcy and with binding of Bet or DMG to the binary Hcy complex. In the presence of CBHcy or Hcy and DMG, W342F and W352F undergo smaller (2 nm) red shifts in their λ_{max} (Table 3) and minimal changes in their IF intensities (Figure 4, panels F and G, respectively) compared to the changes in fluorescence of the WT enzyme when it binds these ligands (Figure 2C,D). It is remarkable that the important reporters of binding at the Bet site are Trp342 and Trp352. Both of these residues, along with Trp331, are located on the dimerization arm of the partner subunit but are relatively close to the Bet binding site, defined from the structure of the CBHcy complex (Figure 9). Trp352 occupies a hydrophobic pocket formed by P268, P269, W279, and E266 (*1*). Trp279 is positioned close to Trp352 and not far from Trp331, where it might quench the fluorescence from these residues, as suggested from the properties of W279F. The shortest distance between Trp352 and the carboxylate group of the Bet analogue is about 8 Å. It is tempting to speculate that elements of the dimerization arm of the neighboring chain move as part of a rearrangement that brings binding groups into position to interact with Bet.

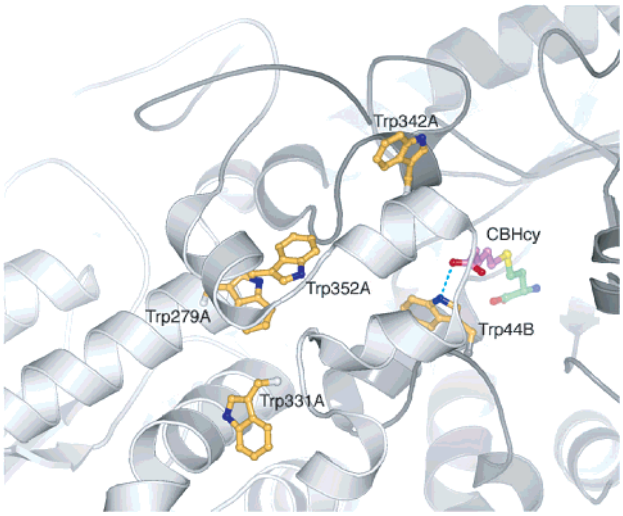

FIGURE 9: Network of tryptophans in proximity to the active site. Tryptophans 44, 279, 331, 342, and 352 are the closest to the active site of BHMT. The above image is magnified and reoriented from Figure 8 and shows the locations of important Trp residues described in the text. CBHcy is shown in pale green (Hcy) and lavender (δ-carboxybutyl).

Preliminary observations of the two crystal structures of human BHMT had led us to speculate that the large changes in IF intensity associated with CBHcy, Hcy/Bet, or Hcy/DMG binding to BHMT could be attributed to Trp44 (*1*). This residue is involved in binding the carboxylate of the Bet analogue and is part of the β1-α1 loop that is disordered in the substrate- and zinc-free (and oxidized) enzyme but clearly visible in the CBHcy complex. It is surprising to find that mutation of Trp44 has such a small effect on the changes in fluorescence that report substrate binding. We continue to believe that changes or movements in this loop, which contacts parts of the dimerization arm, play a role in substrate-induced structural changes. Structures of additional substrate or product complexes will be essential to define the nature and magnitudes of the displacements that are inferred from the fluorescence changes.

The fluorescence changes attributed to residues that are not in contact with substrates provide strong evidence for conformational changes induced by the binding of Hcy and for further changes accompanying the binding of Bet. In agreement with an obligatory order of substrate addition, Bet or DMG alone does not induce any spectral changes. Using equilibrium dialysis with high specific activity [*methyl*-^{14}C]-DMG and at concentrations up to 5 mM, we have confirmed the lack of affinity of this product to BHMT (50 μM) in the absence or presence of saturating concentrations (1 mM) of Met (Collinsová and Garrow, unpublished work). According to the induced-fit hypothesis of Koshland (*10*), the conformational change induced by Hcy would be expected to facilitate assembly of the Bet binding site. The fluorescence changes have provided the first evidence for an induced-fit mechanism for the BHMT reaction or for any of the enzymes that belong to the Hcy methyltransferase family (Pfam 02754).

ACKNOWLEDGMENT

We are grateful to Dr. J. Morgan for reviewing the manuscript before submission.

REFERENCES

1. Evans, J. C., Huddler, D. P., Jiracek, J., Castro, C., Millian, N. S., Garrow, T. A., and Ludwig, M. L. (2002) Betaine-homocysteine methyltransferase: zinc in a distorted barrel, *Structure (Cambridge) 10*, 1159−71.
2. Millian, N. S., and Garrow, T. A. (1998) Human betaine-homocysteine methyltransferase is a zinc metalloenzyme, *Arch. Biochem. Biophys. 356*, 93−8.
3. Matthews, R. G., and Goulding, C. W. (1997) Enzyme-catalyzed methyl transfers to thiols: the role of zinc, *Curr. Opin. Chem. Biol. 1*, 332−9.
4. Breksa, A. P., 3rd, and Garrow, T. A. (1999) Recombinant human liver betaine-homocysteine S-methyltransferase: identification of three cysteine residues critical for zinc binding, *Biochemistry 38*, 13991−8.
5. Peariso, K., Zhou, Z. S., Smith, A. E., Matthews, R. G., and Penner-Hahn, J. E. (2001) Characterization of the zinc sites in cobalamin-independent and cobalamin-dependent methionine synthase using zinc and selenium X-ray absorption spectroscopy, *Biochemistry 40*, 987−93.
6. Evans, J. C., Huddler, D. P., Hilgers, M. T., Romanchuk, G. L., Matthews, R. G., and Ludwig, M. L. (2004) Structures of the N-terminal domains of methionine synthase imply large domain motions during catalysis, *Proc. Natl. Acad. Sci. U.S.A.* (in press).
7. Fromm, H. J., and Nordlie, R. C. (1959) On the purification and kinetic of rat liver thetin-homocysteine transmethylase, *Arch. Biochem. Biophys. 81*, 363−376.
8. Awad, W. M., Jr., Whitney, P. L., Skiba, W. E., Mangum, J. H., and Wells, M. S. (1983) Evidence for direct methyl transfer in betaine:homocysteine S-methyl-transferase, *J. Biol. Chem. 258*, 12790−2.
9. Finkelstein, J. D., Harris, B. J., and Kyle, W. E. (1972) Methionine metabolism in mammals: kinetic study of betaine-homocysteine methyltransferase, *Arch. Biochem. Biophys. 153*, 320−4.
10. Koshland, D. E., Jr. (1958) *Proc. Natl. Acad. Sci. U.S.A. 44*, 98−99.
11. Bose, N., and Momany, C. (2001) Crystallization and preliminary X-ray crystallographic studies of recombinant human betaine-homocysteine S-methyltransferase, *Acta Crystallogr. D: Biol. Crystallogr. 57*, 431−3.
12. Eftink, M. R. (1997) Fluorescence methods for studying equilibrium macromolecule-ligand interactions, *Methods Enzymol. 278*, 221−57.
13. Segel, I. (1975) *Enzyme Kinetics: Behaviour and analysis of rapid equilibrium and steady-state enzyme systems*, John Wiley & Sons, New York.
14. Garrow, T. A. (1996) Purification, kinetic properties, and cDNA cloning of mammalian betaine-homocysteine methyltransferase, *J. Biol. Chem. 271*, 22831−8.
15. Hanes, C. S. (1932) *Biochem. J. 26*, 1406−1421.
16. Callis, P. R. (1997) 1La and 1Lb transitions of tryptophan: applications of theory and experimental observations to fluorescence of proteins, *Methods Enzymol. 278*, 113−50.
17. Skiba, W. E., Taylor, M. P., Wells, M. S., Mangum, J. H., and Awad, W. M., Jr. (1982) Human hepatic methionine biosynthesis. Purification and characterization of betaine: homocysteine S-methyltransferase, *J. Biol. Chem. 257*, 14944−8.
18. Allen, R. H., Stabler, S. P., and Lindenbaum, J. (1993) Serum betaine, *N*,*N*-dimethylglycine and *N*-methylglycine levels in patients with cobalamin and folate deficiency and related inborn errors of metabolism, *Metabolism 42*, 1448−60.
19. Ericson, L. (1960) Betaine-Homocysteine-Methyl-Transferases. I. Distribution in Nature, *Acta Chem. Scand. 14*, 2127−2134.
20. McGregor, D. O., Dellow, W. J., Lever, M., George, P. M., Robson, R. A., and Chambers, S. T. (2001) Dimethylglycine accumulates in uremia and predicts elevated plasma homocysteine concentrations, *Kidney Int. 59*, 2267−72.
21. Gonzalez, B., Campillo, N., Garrido, F., Gasset, M., Sanz-Aparicio, J., and Pajares, M. A. (2003) Active-site-mutagenesis study of rat liver betaine-homocysteine S-methyltransferase, *Biochem J. 370*, 945−52.
22. Vivian, J. T., and Callis, P. R. (2001) Mechanisms of tryptophan fluorescence shifts in proteins, *Biophys J. 80*, 2093−109.

BI049821X